Diagnostic and Interventional Imaging 000 (2023) 1–10

Original article

What is the benefit of gadolinium-chelate injection for the diagnosis of local recurrence of clear cell renal cell carcinoma after percutaneous thermal ablation with MRI?

Julien Gay Depassier[a,1], Amandine Crombé[a,b,1], Eva Jambon[a], Jean Christophe Bernhard[c], Yann Le Bras[a], Nicolas Grenier[a,b], Clément Marcelin[a,d,*]

[a] *Centre Hospitalier Universitaire (CHU) de Bordeaux, Department of Radiology, Hôpital Pellegrin, 33076 Bordeaux, France*
[b] *Models in Oncology (MONC) Team, INRIA Bordeaux Sud-Ouest, CNRS UMR 5251 & Bordeaux University, 33400, Talence, France*
[c] *Centre Hospitalier Universitaire (CHU) de Bordeaux, Deparment of Urology, Hôpital Pellegrin, 33400 Bordeaux, France*
[d] *Bordeaux Institute of Oncology, BRIC U1312, INSERM, Université de Bordeaux, 33000 Bordeaux, France*

ARTICLE INFO

Index terms:
Clear cell renal cell carcinoma
Contrast media
Cryosurgery
Magnetic resonance imaging
Radiofrequency ablation
Renal tumor

ABSTRACT

Purpose: The purpose of this study was to compare the diagnostic capabilities of contrast-enhanced (CE)-MRI to those of non-CE-MRI to diagnose local recurrence of clear cell renal cell carcinoma (ccRCC) after percutaneous thermal ablation (TA).

Materials and methods: This institutional, review board-approved, case-control, single-center retrospective study included all consecutive adult patients with at least two post-TA MRIs showing local recurrence of ccRCC after TA validated by multidisciplinary board. 'Control' patients without recurrence were randomly-selected with a case:control ratio of 2/3. Four senior radiologists reviewed in a double-blinded fashion non-CE sequences of last two consecutive MRI examinations (non-CE-MRIs), assessed the presence of recurrence of ccRCC, then reviewed the CE sequences (CE-MRI) and determined again the presence of a recurrence. Area under the receiver operating characteristic curve (AUROC), sensitivity, specificity and accuracy were compared for each reader for non-CE-MRI and CE-MRI.

Results: Fifty-one patients (41 men; mean age, 77.5 years) who underwent percutaneous TA for ccRCC were included. There were a total of 21 recurrences and 35 scars. Whoever the reader, AUROC was not significantly different (mean, 0.86 with-CE-MRI *vs.* 0.81 with non-CE-MRI; *P* values ranging between 0.08 and 0.98), neither sensitivity (mean, 76.2% with CE-MRI *vs.* 71.4% with non-CE-MRI; *P* values ranging between 0.06 and >0.99), nor accuracy (85.8% with CE-MRI *vs.* 80.8% with non-CE-MRI; *P* values ranging between 0.07 and >0.99). Change in specificity depended on the reader with a significant increase for one reader (+20%; $P = 0.02$) and a significant decrease for another reader (-17.2%; $P = 0.03$).

Conclusion: Non-CE MRI has good diagnostic performance for the follow-up of patients with ccRCC treated using percutaneous TA, questioning the systematic use of GBCA injection.

1. Introduction

Most newly-diagnosed renal cancers are localized (*i.e.*, stage I-II, 60–70%) and approximately 76% clear cell renal cell carcinomas (ccRCC) [1,2]. Imaging guided percutaneous thermal ablations (TAs) such as radiofrequency ablation, cryoablation and microwave ablation are now clearly mentioned as valid alternatives to surgery for patients with T1 renal cancers < 3 cm according to the latest guidelines from the American Urological Associations. The European Association of Urology, the European Society of Medical Oncology, the French Urological Association or the Cardiovascular and Interventional Radiological Society of Europe recommend these treatments as alternatives for patients not fit for surgery, and those with important comorbidities [3–6]. Several studies and meta-analyses have reported lower rates of complications, preservation of the renal function, similar metastatic recurrence free and overall survivals, but with a slightly greater recurrence rate [7–15]. Regular follow-up of

Abbreviations: AUROC, Area under the receiver operating characteristic curve; CI, Confidence interval; ccRCC, Clear cell renal cell carcinoma; CE, Contrast-enhanced; GBCA, Gadolinium-based contrasts agent; LD, Longest diameter; ROC, Receiver operating characteristic; SD, Standard deviation; TA, Thermal ablation

* Corresponding author:
E-mail address: clement.marcelin@gmail.com (C. Marcelin).

[1] These authors contributed equally to this paper and share 1st co-authorship

https://doi.org/10.1016/j.diii.2023.06.003
2211-5684/

Please cite this article as: J. Gay Depassier, A. Crombé, E. Jambon et al., What is the benefit of gadolinium-chelate injection for the diagnosis of local recurrence of clear cell renal cell carcinoma after percutaneous thermal ablation with MRI?, Diagnostic and Interventional Imaging (2023), https://doi.org/10.1016/j.diii.2023.06.003

patients treated with TAs using cross-sectional imaging is mandatory to rapidly detect and treat incomplete TA with residual disease and/or local recurrence [16].

Typically, ablation zones without recurrence (also named 'scars') are characterized by a heterogenous signal, disappearance of contrast enhancement and progressive decrease in longest diameter (LD). On the opposite, an increase in size of the ablation zone, and appearance of a nodular or crescent-like lesion on contrast-enhanced (CE) imaging examination should raise suspicion for local recurrence [17–20]. Consequently, follow-up MRI after renal TA routinely includes the use of intravenous administration of a gadolinium-based contrast agent (GBCA) and comparative evaluations until five years after treatment [17,21,22].

Yet, the benefit of the use of GBCA for the follow-up of patients with ccRCC treated using percutaneous TA has never been clearly addressed. Initially, most follow-up examinations were performed with CT, which demonstrates lower spontaneous tissue contrast compared to MRI, making mandatory the intravenous administration of iodinated contrast material, which is not free from side-effects [23]. On the opposite, MRI conveys good contrast resolution and high tissue characterization capabilites on non-CE sequences. Nevertheless, post-TA follow-up MRI protocols always include multi-parametric imaging, including non-CE and CE sequences [21]. Furthermore, since few years, several animal and human studies have demonstrated the presence of GBCA deposits in central and peripheral neurologic structures, skin, liver or kidney, especially with linear agents, of which the long-term effects remain under scrutiny [24–27]. Furthermore, after excretion from the patient's body via the urinary tract, gadolinium is responsible for contamination that have now be proven in environmental samples [28]. Lastly, in some situations GBCA cannot be injected, in particular in patients with prior allergy to GBCA or in pregnant women [29].

Therefore, given this uncertainty about the impact of repetitive GBCA administration in addition to the environmental aspect and its technical implications in terms of patients' preparation and examination duration, the purpose of this study was to assess and compare the diagnostic performances and inter-observer reproducibility of non-CE to those of CE MRIs after percutaneous TA for ccRCC.

2. Material and methods

2.1. Study design

This single-center retrospective case-control study was approved by our Committee for Persons Protection (approval number: DC-2012/108) and by our institutional review board (approval number: DR-2013-206). The need for written consent was waived due to the retrospective nature of the study.

Patients were identified from the French UroCCR national database (NCT03293563), which collects clinical, biological, radiologic treatment and follow-up data from patients with newly diagnosed renal cancers (www.uroccr.fr). From this database, all consecutive adult patients with local recurrence following percutaneous TA (cryoablation, microwave and radiofrequency, performed in agreement with the guidelines) of ccRCC in our tertiary referral center form January 2010 to January 2020, diagnosed by radiologists during follow-up and validated by the multidisciplinary tumor board of our institution, were extracted. Only patients with ccRCC were included. For all patients, a definite diagnosis of ccRCC was made using histopathological analysis.

For all patients, inclusion criterion was the availability of two consecutive CE MRIs of good quality after TA (MRI-0 and MRI-1) for a newly diagnosed lesion. The MRI examination on which the diagnosis of local recurrence was achieved and the previous MRI examination were selected. Regarding the 'recurrence' cohort, additional inclusion criterion was diagnosis of post-TA local recurrence on imaging (defined as an unequivocally appearing or growing nodule or thickening showing high signal intensity on T2-weighted images and contrast enhancement during the follow-up MRIs) [30]. All relapses were validated by the multidisciplinary tumor board of our institution. Inclusion of multiple recurrences per patient was not allowed. The 'control' cohort was built by randomly-choosing the same number of patients (rounded to the upper ten) in the groups of patients from the uroCCR database without post-TA relapse who fulfilled the inclusion criteria. If more than two control CE-MRIs were available, the latest two MRI examinations were chosen. Exclusion criteria included Von Hippel Lindau disease, renal tumor other than ccRCC and recurrence diagnosed on first follow-up MRI (which rather corresponded to incomplete TAs). Fig. 1 shows the study flow-chart.

Patients' sex and age, Fuhrman grade and the TA technique used were collected from medical reports. Additionally, the pre-treatment imaging (CE-CT or CE-MRI) was reviewed to collect the tumor LD, its location on axial image (*i.e.*, exophytic, endophytic, endosinusal or mixed) and on orthogonal plane (upper, equatorial and lower pole), and the presence of tumor enhancement on the arterial phase (*i.e.*, hyperarterialization).

2.2. MRI aprotocol

Examinations were performed on 1.5 and 3-Tesla magnets from our center. The protocol included axial Dixon T1-weighted imaging or in-phase / out-of-phase and axial and coronal T2-weighted (with or without fat suppression), one axial or coronal diffusion-weighted imaging with mono-exponential apparent diffusion coefficient parametric map, one axial dynamic acquisition after GBCA injection (acquisition at 30 s, 90 s, 180 s and 5 min) with fat signal suppression and subtraction technique reconstruction. Table 1 summarizes the acquisition parameters for each MR-system. Diffusion-weighted imaging was missing (or non-analyzable) for seven examinations, subtraction reconstruction for two examinations and dynamic acquisition after injection was not available for one examination. The GBCA used for MRI follow-up were: Dotarem® (0.5 mmol/L, gadoterate meglumine, Guerbet) for 44/102 MRIs (43.3%), followed by Clariscan® (0.5 mmol/L, gadoterate meglumine, GE Healthcare), Prohance® (0.5 mmol/L, gadoteridol, Bracco Imaging) and Gadovist® (1 mmol/L, Gadobutrol, Bayer Healthcare) used equally (10/102 MRIs [9.8%] for each of them). The specific GBCA remained unknown for 36/102 MRIs (35.3%).

2.3. MRI analysis

For each treated patients, both MRIs were pseudonymized and stored on a specific data space of our picture archiving and communication system (PACS, Carestream, Carestream Health,) and duplicated to two examinations only containing sequences without contrast injection (non-CE-MRI) and two examinations containing all sequences (CE-MRI).

Four senior radiologists reviewed the entire datasets (non-CE-MRI and CE-MRI) blinded to each other and to patients' data and outcome, namely Reader-1 (A.C.) with four years experiences in oncologic imaging, Reader-2 (E.J.) with four years experiences in urogenital imaging, Reader-3 (N.G.) with 25 years experiences in urogenital imaging and Reader-4 (C.M.) with five years experiences in urogenital imaging.

The MRI readings were achieved as follows for each patient: the radiologist opened the two consecutive non-CE-MRIs side-by-side and had to assess whether a recurrence was present, uncertain, or present on the latest after comparing the two, and then which sequence(s) was the most determining for her/his analysis. Afterwards, without delay, the radiologist opened the two consecutive CE-MRIs side-by-side and assessed whether a recurrence was present, absent or uncertain, and, final, which sequence(s) was the most

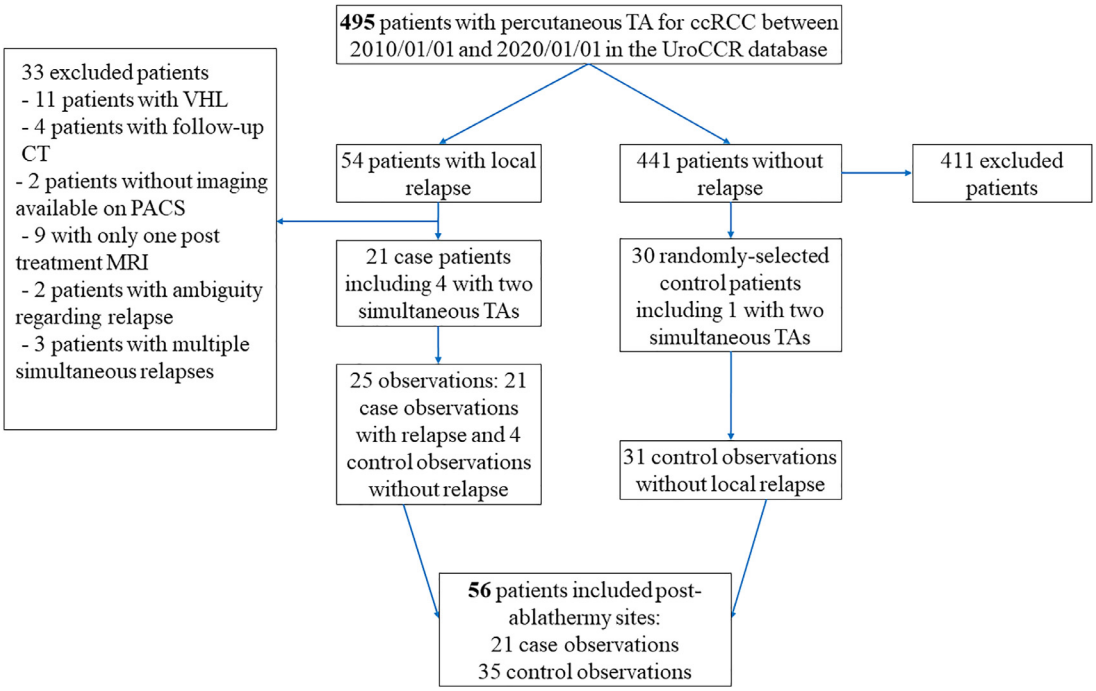

Fig. 1. Study flowchart.
ccRCC: clear cell renal cell carcinoma, VHL: Von Hippel Lindau disease.

determining. Regarding patients with two treated sites (four patients from the 'case' cohort and one patient from the 'control' cohort) each site was analyzed separately.

Moreover, one senior reader (Reader-1) also reported the LD of the ablation zones, its signal on T1 and T2-weighted images (categorized as low, intermediate, high and heterogeneous compared to normal renal parenchyma), the presence of a peripheral halo with low signal intensity on T2-weighted images surrounding the ablation zone, and the enhancement of this zone. After revealing the ablation zone with recurrence, reader-1 also measured the LD of the recurrence, its shape (categorized as crescent or nodular), it signals on T1- and T2-weighted images, its apparent diffusion coefficient values value and its enhancement pattern (categorized as peak-then-washout, peak-then-plateau and no-peak-progressive)

2.4. Statistical analysis

Statistical analyses were performed with R (v4.1.0, Vienna, Austria) by A.C. (PhD in applied mathematics, with three years of experience as a senior researcher in computational medicine). All tests were two-tailed. A P-value < 0.05 was considered to indicate significant difference.

Quantitative variables were expressed as mean ± standard deviation (SD) and range, or median, Q1-Q3 and range, depending on the Shapiro-Wilk normality test [30]. Qualitative variables were expressed as raw numbers, proportions and percentages. Patient's and initial tumor's characteristics were compared between the 'recurrence' group and the 'control' group to search for differences. For association with qualitative variable, the Chi-square or Fischer exact test were used, as appropriate. For association with quantitative variable, Student t-test or Mann Whitney test for unpaired date were used depending on normality of the distribution.

For each radiologist and each setting (non-CE-MRI, CE-MRI), the area under the receiver operating characteristic curve (AUROC) was estimated with 95% confidence interval (CI) ('pROC' R package) [31]. The AUROC for non-CE-MRI and CE-MRI were compared using paired Delong tests. After dichotomizing the radiological assessment into 'negative' *vs.* 'uncertain or positive', the sensitivity, specificity, accuracy (true positive and true negative divided by the total number of observations) were calculated with their 95% CIs and compared using

Table 1
Parameters of MRI sequences.

Sequence	Acquisition plane	TE (ms)	TR (ms)	Flip angle (°)	Matrix	FOV (mm^2)	Thickness (mm)
1.5 Tesla							
T2W 2D TSE	Axial	80	2141	90	384	350 × 350	3
T2 2D WTSE	Coronal	80	1448	90	384	350×350	3
DWI (b100–400–800)	Axial	69	3932	90	240	345×276	5
T1W 2D IPOP	Axial	2.3/4.6	211	75	320	400×330	6
T1W 2D FS Thrive	Axial	1.87	3.9	10	480	365×298	4
3 Tesla							
T2 2D FSE	Axial	160	15,200	142	512	360×288	4
T2W 2D FS FSE	Coronal	80	12,510	111	512	380×380	4
Diffusion (b100–400–800)	Axial	70	5000	90	256	400×400	5
T1W 2D IP-OP	Axial	1.3/2.5	5.0	12	512	400×320	3.4
T1W 2D LAVA Flex	Axial	1.9	5.4	12	512	400×320	3.4

2D indicates two-dimensional; DWI indicates diffusion-weighted imaging; FS indicates fat-suppressed; FSE indicates fast spin-echo; FSPGR indicates fast spoiled gradient-echo; FOV indicates field of view; IP-OP indicates In-phase and out-of-phase); TE indicates echo time; TR indicates repetition time; T1W indicates T1-weighted; T2W indicates T2-weighted; TSE indicates turbo spin-echo.

McNemar test ('DTComPair' R package). The mean sensitivity, specificity, accuracy and AUROC over the four radiologists were also calculated for non-CE-MRI and CE-MRI.

The inter-observer reproducibility for the radiological assessment (*i.e.*, an ordinal variable with three categories: absent < uncertain < present) on non-CE-MRI and on CE-MRI over four readers who interpreted the same dataset was evaluated using the Krippendorff's alpha (α_K) for ordinal variables, which ranged from −1 (complete disagreement) to +1 (absolute agreement) ('irr' R package). The 95% CIs of α_K for non-CE-MRI and CE-MRI were estimated using bootstrapping on 10,000 replicates of the study population. To test whether the inter-rater reproducibility was significantly different, the *P*-value was inferred from the 95% CI of their bootstrapped differences ('boot' R package).

After putting side-by-side the conclusion on non-CE-MRI, CE-MRI and the gold-standard, a new variable named 'Diagnostic improvement with CE' was encoded, from which the added value of the use of GBCA was inferred (when a misdiagnosis was corrected with injection, *vs.* same diagnosis with GBCA or correct diagnosis with non-CE-MRI changed to misdiagnosis with CE-MRI), as summarized in Table 2. Hence, the number and percentage of situations for which the use of GBCA (*i.e.*, CE-MRI) improved the final diagnosis was counted for each reader.

To better understand the features of recurrences that benefited from injection *vs.* those that did not, recurrences that were correctly diagnosed on non-CE-MRI, and recurrences that were misdiagnosed on non-CE-MRI but correctly diagnosed on CE-MRI by at least three out of four readers were filtered. Their clinical, pathological and radiological features on pre-treatment examination and on the CE-MRI of the recurrence were compared by using unpaired Wilcoxon tests (for quantitative variables and Fisher or Chi-square test for categorical variables.

3 Results

3.1. Patients' characteristics

Characteristics of patients, initial ccRCC, procedures and MRI follow-up are reported in Table 3. Fifty-four out of the 495 patients (10.9%) treated at our center and included in the UroCCR database between January 2010 and January 2020 showed a local recurrence. Twenty-one recurrences were finally included (Fig. 1) in 21 patients, of whom four underwent a second simultaneous ablation session. Thirty 'control' patients meeting the inclusion criteria were randomly sampled in the 441/495 (89.1%) remaining patients without post-TA recurrence including one patient with two procedures. Thus, the 'control' cohort comprised 35 TA procedures and the 'recurrence' cohort 21 TA procedures, for a total of 51 patients and 102 MRI examinations. There were 41 men and 10 women, with a mean age of 77.5 ± 10.3 (SD) years (range: 50–95 years). There were 21 patients with a recurrence, four patients with a recurrence and a scar, 29 patients with a scar and one patient with two scars.

Regarding ccRCCs and procedures, the median delay between the two post-TA MRIs was 12 months (Q1, Q3: 4.4, 12.3; range: 2.7–24 months). Most initial ccRCCs were Fuhrman grade 2 (34/41, 82.9%, 15 patients with missing data) with a mean LD of 28 ± 9 (SD) mm (range: 13–52 mm) and showed hyperarterialization on pre-treatment imaging (42/52, 80.8%, four patients with non-analyzable data). Ablation techniques included cryoablation for 16/56 (33.9%) procedures, microwave ablation for 6/56 (10.7%) procedures and radiofrequency ablation for 31/56 (55.4%) procedures. For each of these characteristics, there were no significant differences between the recurrence cohort and the control cohort (Table 3).

3.2. Comparisons of diagnostic performances

No differences in AUROC were found between MRI-CE and non-CE MRI (*P*-value range: 0.08–0.98). The mean AUROC was 0.81 with non-CE-MRI (from 0.74 [95% CI: 0.61–0.87] for Reader-3 to 0.84 [95% CI: 0.73–0.94] for Reader-2) *vs.* 0.86 with CE-MRI (from 0.82 [95% CI: 0.71–0.93] for Reader-4 to 0.93 [95% CI: 0.85–1] for Reader-2) (Table 4) (Fig. 2).

When considering uncertain assessment as positive, no differences in sensitivity were found between CE-MRI and non-CE-MRI for all readers (same for Reader-3 and Reader-4, +23.8% for Reader-1 and +19.1% for Reader-2; *P*-value range: 0.06–1). The mean sensitivity was 71.4% with non-CE-MRI (from 66.7% [95% CI: 43–85.4%] for Reader-3 to 76.2% [95% CI: 52.8–91.8%] for Reader-4) *vs.* 82.2% with CE-MRI (from 66.7% [95%CI: 43–85.4%] for Reader-3 to 95.2% [95% CI: 76.2–99.9%] for Reader-1) (Fig. 3).

Table 2
Definitions of diagnostic improvement and added value of gadolinium-based contrast agent.

True diagnosis	Assessment on unenhanced MRI	Assessment on CE-MRI	Diagnostic improvement with GBCA	Added value of GBCA
No recurrence	Recurrence	Recurrence	No, same misdiagnosis	No
		Uncertain	Yes, (half) downgrading of a scar	**Yes**
		No recurrence	Yes, downgrading of a scar	**Yes**
	Uncertain	Recurrence	No, incorrect upgrading of scar	No
		Uncertain	No, same misdiagnosis	No
		No recurrence	Yes, downgrading of a scar	**Yes**
	No recurrence	Recurrence	No, incorrect upgrading of scar	No
		Uncertain	No, incorrect upgrading of scar	No
		No recurrence	No, same correct diagnosis	No
Recurrence	Recurrence	Recurrence	No, same correct diagnosis	No
		Uncertain	No, incorrect downgrading of a recurrence	No
		No recurrence	No, incorrect downgrading of a recurrence	No
	Uncertain	Recurrence	Yes, upgrading of a recurrence	**Yes**
		Uncertain	No, same misdiagnosis	No
		No recurrence	No, incorrect downgrading of a recurrence	No
	No recurrence	Recurrence	Yes, upgrading of a recurrence	**Yes**
		Uncertain	Yes, (half) upgrading of a recurrence	**Yes**
		No recurrence	No, same misdiagnosis	No

Added value for GBCA was considered when the diagnosis was already correct before reading contrast-enhanced MRI sequences.
Upgrading consists of changes from no recurrence-to-uncertain, no recurrence-to-recurrence, and uncertain-to-recurrence in the reading when using GBCA.
Downgrading consists of changes from recurrence-to-uncertain, recurrence-to-no-recurrence and uncertain-to-no recurrence in the reading when using GBCA.
CE indicates contrast-enhanced; GBCA indicates gadolinium-based contrast agent.

Table 3
Characteristics of 51 patients with 56 clear cell renal carcinomas treated with percutaneous thermal ablation.

Characteristics	All	Case cohort	Control cohort	*P*-value
Patients	***n* = 51**	***n* = 21**	***n* = 30**	
Age (years)	77.5 ± 10.3 [50–95]	74.7 ± 6.8 [57.9–84.1]	72.8 ± 11.7 [45.3–92]	0.47
Sex				> 0.99
Male	41/51 (80.4)	17/21 (80.9)	24/30 (80)	
Female	10/51 (19.6)	4/21 (19)	6/30 (20)	
Tumors	***n* = 56**	***n* = 25**	***n* = 31**	
Fuhrman Grade*				0.69
I	2/41 (4.9)	1/18 (5.6)	1/23 (4.3)	
II	34/41 (82.9)	14/18 (77.8)	20/23 (87)	
III	4/41 (9.8)	2/18 (11.1)	2/23 (8.7)	
IV	1/41 (2.4)	1/18 (5.6)	0/23 (0)	
Tumor longest diameter (mm)	28 ± 9 [13–52]	28 ± 10 [13–52]	27 ± 9 [13–46]	0.52
Tumor side				> 0.99
Right	28/56 (50)	10/21 (47.6)	18/35 (51.4)	
Left	28/56 (50)	11/21 (52.4)	17/35 (48.6)	
Tumor location (depth)				0.63
Endophytic - endosinusal	20/56 (37.1)	8/21 (38.1)	12/35 (34.3)	
Endophytic	3/56 (5.4)	2/21 (9.5)	1/35 (2.9)	
Endophytic and exophytic	26/56 (46.4)	8/21 (38.1)	18/35 (51.4)	
Exophytic	7/56 (12.5)	3/21 (14.3)	4/35 (11.4)	
Tumor location (height)				0.96
Upper side	15/56 (26.8)	5/21 (23.8)	10/35 (28.6)	
Upper side - equatorial	2/56 (3.6)	1/21 (4.8)	1/35 (2.9)	
Equatorial	25/56 (44.5)	9/21 (42.9)	16/35 (45.7)	
Equatorial - lower side	3/56 (5.4)	1/21 (4.8)	2/35 (5.7)	
Lower side	11/56 (19.6)	5/21 (23.8)	6/35 (17.1)	
Tumor location (ante-posterior)*				0.06
Anterior	16/53 (30.2)	3/20 (15)	13/33 (39.4)	
Medial	17/53 (32.1)	10/20 (50)	7/33 (21.2)	
Posterior	20/53 (37.7)	7/20 (35)	13/33 (39.4)	
Hyper-arterialized tumors*				0.98
No	10/52 (19.2)	4/18 (22.2)	6/34 (17.6)	
Yes	42/52 (80.8)	14/18 (77.8)	28/34 (82.4)	
Type of percutaneous TA				0.63
Cryoablation	19/56 (33.9)	8/21 (38.1)	11/35 (31.4)	
Microwave	6/56 (10.7)	3/21 (14.3)	3/35 (8.6)	
Radiofrequency	31/56 (55.4)	10/21 (47.6)	21/35 (60)	

NOTE- Quantitative variables are expressed as means ±standard deviations; numbers in brackets are ranges. Qualitative variables are expressed as proportions followed by percentages into parentheses.
* There were 15 patients without available grade, three patients without available data about the initial exact tumor location, and four patients without available data regarding tumor hyper-arterialization on pre-treatment MRI.
TA: thermal ablation.

The specificity decreased with CE-MRI compared to non-CE-MRI for Reader-1 (−17.2%; *P* = 0.03), stayed not different for Reader-2 (−5.7%; *P* = 0.3173), and Reader-4 (+2.9%; *P* = 0.56) and increased with CE-sequences for Reader-3 (+20%; *P* = 0.02). The mean specificity was 86.4% with non-CE-MRI (from 77.1% [95% CI: 59.9 −89.6%] for Reader-3 to 94.3% [95% CI: 80.8–99.3%] for Reader-2) *vs.* 86.4% with CE-MRI (from 71.4% [95% CI: 53.7–85.4%] for Reader-1 to 97.1% [95% CI: 85.1–99.9%] for Reader-3).

Table 4
Diagnostic performance metrics without and with gadolinium chelates injection over the four independent readers.

Diagnostic performance metrics	Radiologist	Non-CE-MRI	CE-MRI	*P*-value
AUROC	Reader-1	0.83 (0.71–0.94)	0.85 (0.77–0.94)	0.69
	Reader-2	0.84 (0.73–0.94)	0.93 (0.85–1)	0.07
	Reader-3	0.74 (0.61–0.87)	0.83 (0.72–0.94)	0.18
	Reader-4	0.82 (0.71–0.93)	0.82 (0.71–0.93)	0.97
Sensitivity (%)	Reader-1	71.4 (47.8–88.7)	95.2 (76.2–99.9)	0.05
	Reader-2	71.4 (47.8–88.7)	90.5 (69.6–98.8)	0.15
	Reader-3	66.7 (43–85.4)	66.7 (43–85.4)	>0.99
	Reader-4	76.2 (52.8–91.8)	76.2 (52.8–91.8)	>0.99
Specificity (%)	Reader-1	88.6 (73.3–96.8)	71.4 (53.7–85.4)	**0.03***
	Reader-2	94.3 (80.8–99.3)	88.6 (73.3–96.8)	0.31
	Reader-3	77.1 (59.9–89.6)	97.1 (85.1–99.9)	**0.01***
	Reader-4	85.7 (69.7–95.2)	88.6 (73.3–96.8)	0.56
Accuracy (%)	Reader-1	82.1 (69.6–91.1)	80.4 (67.6–89.8)	>0.99
	Reader-2	85.7 (73.8–93.6)	89.3 (78.1–96)	0.77
	Reader-3	73.2 (59.7–84.2)	85.7 (73.8–93.6)	0.07
	Reader-4	82.1 (69.6–91.1)	83.9 (71.7–92.4)	>0.99

AUROC indicates area under the ROC curve; CE indicates contrast-enhanced. Numbers in parentheses are 95% confidence intervals.
* $P < 0.05$. Significant results are in bold.

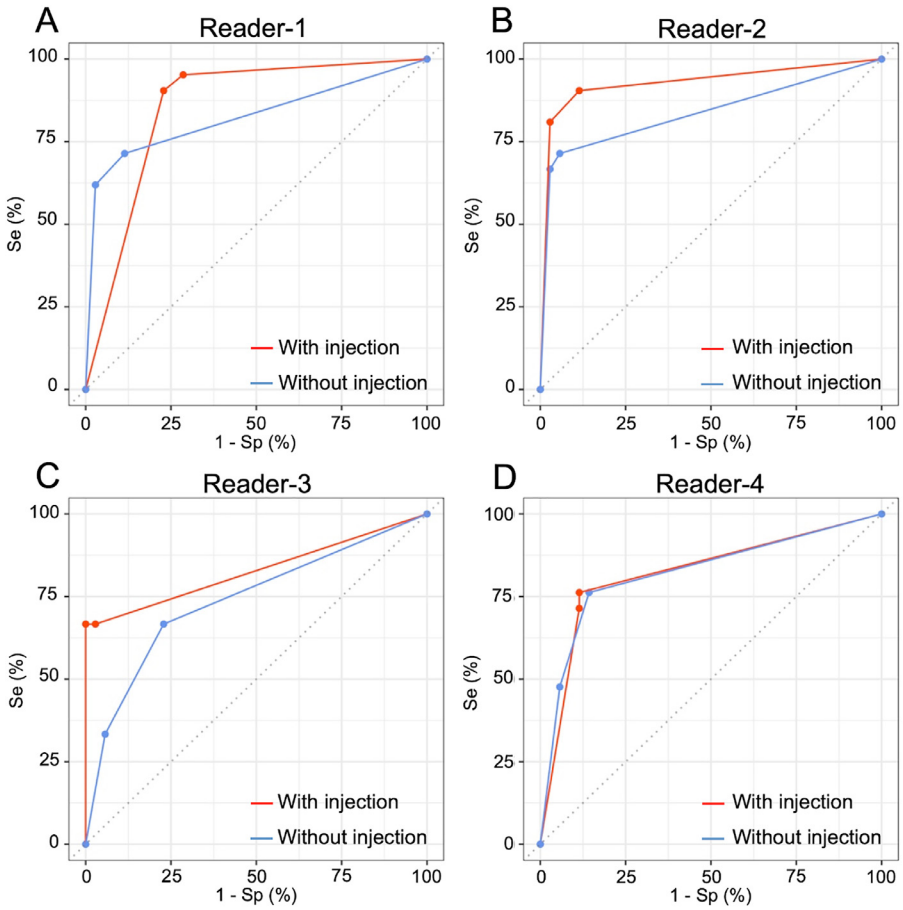

Fig. 2. Graphs show the receiver operating characteristic (ROC) curve analysis without and with gadolinium-chelate injection for Reader-1 (**A**), Reader-2 (**B**), Reader-3 (**C**) and Reader-4 (**D**). Se: sensitivity; Sp: specificity.

No significant differences in accuracy were found between CE-MRI and non-CE-MRI (*P*-value range: 0.07–> 0.991). The mean accuracy was 80.8% with non-CE-MRI (from 73.2% [95% CI: 59.7–84.2%] for Reader-3 to 85.7% [95% CI: 73.8–93.6%] for Reader-2) *vs.* 84.8% with CE-MRI (from 80.4% [95% CI: 67.6–89.8%] for Reader-1 to 89.3% [95% CI: 78.1–96%] for Reader-2).

Before analyzing CE-MRI, the most helpful MRI sequence to achieve a correct diagnosis of recurrence was the T2-weighted sequence for 10/15 (66.7%) true-positives for Reader-1, 13/15 (86.7%) true-positives for Reader-2, 4/14 (28.5%) true-positives for Reader-3, and 15/16 (93.8%) true-positives for Reader-4. After the reading of CE-MRI dataset, the radiologists rated CE-MRI sequences as the most helpful in 14/20 (70%) true-positives for Reader-1, 16/19 (84.2%) true-positives for Reader-2, 14/14 (100%) true-positives for Reader-3 and 12/16 (75%) true-positives for Reader-4.

3.3. Comparisons of inter-observer reproducibility

The α_K for non-CE-MRI was 0.44 (95% CI: 0.29–0.62; indicating fair inter-observer reproducibility) *vs.* 0.60 for CE-MRI (95% CI: 0.46–0.76; indicating moderate inter-observer reproducibility), with no differences ($P = 0.08$).

3.4. Changes in diagnosis secondary to the use of GBCA

The use of GBCA enabled to correct false-negatives or uncertain assessments for 8/21 (38.1%) recurrences with Reader-1, 6/21 (28.6%) recurrences with Reader-2, 8/21 (38.1%) recurrences with Reader-3 and 5/21 (23.8%) recurrences with Reader-4 (average over the four readers: 32.2%) (Table 5). The use of GBCA enabled to correct false-positives or uncertain assessments for 1/35 (2.9%) scar with Reader-1, 1/35 (2.9%) scar with Reader-2, 8/35 (22.9%) scars with Reader-3 and 2/35 (5.7%) scars with Reader-4 (average over the four readers: 8.6%).

The use of GBCA was responsible for the downgrading of a true recurrence for 2/21 (9.5%) recurrences with Reader-1, 3/21 (14.3%) recurrences with Reader-2, 1/21 (4.8%) recurrence for Reader 3 and none with Reader 4 (average over the four readers, 7.1%). Finally, the use of GBCA failed to correct a misdiagnosis (false-positive or false-negative) for 2/56 (3.6%) procedures with Reader-1, 1/56 (1.8%) procedure with Reader-2, 6/56 (10.7%) procedures with Reader-3, and 7/56 (12.5%) procedures with Reader-4 (average over the four readers, 7.1%).

Therefore, the use of GBCA provided an added value in 9/56 (16.1%) procedures for Reader-1, 7/56 (12.6%) procedures for Reader-2, 16/56 (28.6%) procedures for Reader-3 and 7/56 (12.5%) procedures for Reader-4 (average over the four readers, 17.5%).

Figs. 4 and 5 show recurrences correctly diagnosed with CE-MRI and non-CE-MRI, respectively. Fig. 6 shows a simple scar correctly diagnosed by all radiologists without uncertainty thanks to the use of GBCA.

No significant differences were found regarding the characteristics of the initial tumor, treated site and relapse in patients who relapsed depending on whether the correct diagnosis required the use of GBCA ($n = 8$) or not ($n = 8$) in a consensual reading (Table 6).

4. Discussion

In this study, we found that the diagnostic performances of four radiologists are good either using non-CE-MRI or CE-MRI, suggesting

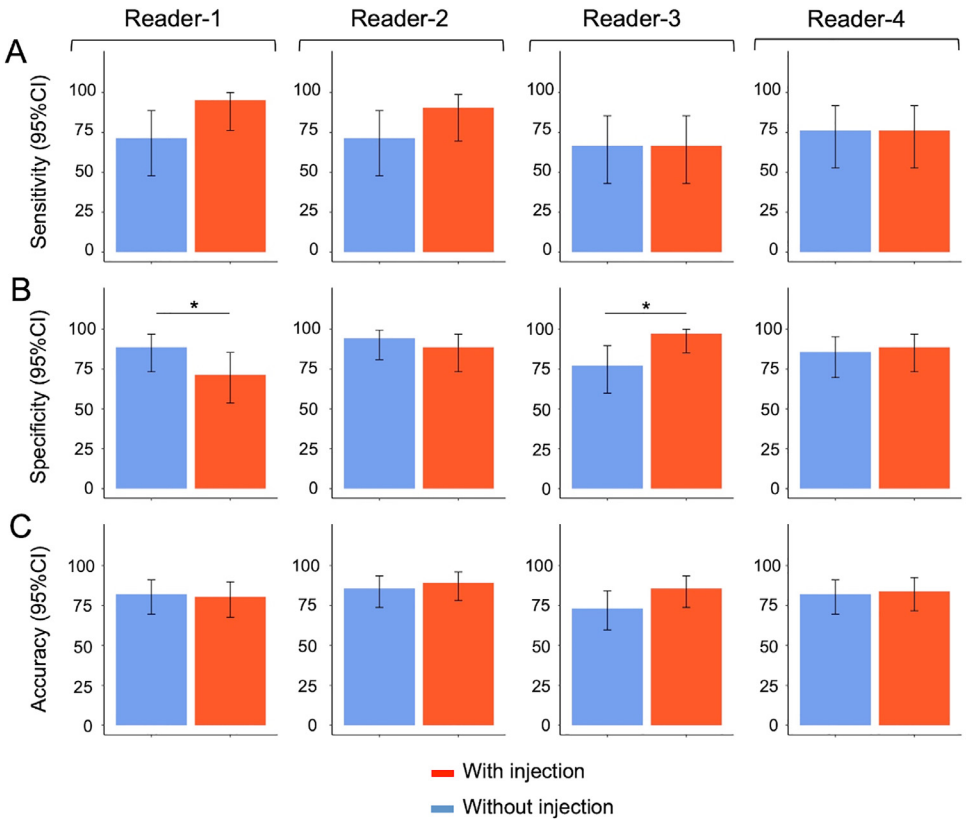

Fig. 3. Graphs show results of the comparison of sensitivities (**A**), specificities (**B**) and accuracies (**C**) without and with gadolinium-based contrast agent over four independent readers, with 95% confidence interval (CI).

a limited incremental value for GBCA in terms of sensitivity, specificity and accuracy (+10.8%, +0% and +4% on average, respectively). However, a closer look to individual performances show that changes in specificity and accuracy are variable and depend on the radiologists. This suggests heterogeneous methods for interpreting post-TA MRIs as some radiologists may increase their sensitivity with the use of GBCA (herein, Reader-1 and Reader-2), whereas others may increase their specificity (herein, Reader-3). Finally, other readers may show constant performances with and without injection (herein, Reader-4). Thus, the interpretation of those follow-up MRIs would benefit from the harmonization of MRI reading, an assessment of the predictive value of each radiological feature, and a standardized reporting system.

Interestingly, the inter-observer reproducibility to diagnose recurrence was better when using GBCA. The comparison almost reaches significance, which could reflect that using CE images reduces uncertainty and facilitates diagnosis. To our knowledge, reproducibility analyses of MRI to diagnose post-TA recurrence has never been performed although it is mandatory to validate any biomarker.

The detailed analysis of the added value of intravenous administration of GBCA also showed that the benefit of additional CE sequences mostly relates to the diagnosis of recurrence (*i.e.*, upgrading a false negative with non-CE-MRI to a true positive with CE-MRI, occurring for eight, six, eight and five out of 21 recurrences across the four radiologists). Conversely, the added value of GBCA to

Table 5
Assessment of the added value of gadolinium based contrast agent to make the correct final diagnosis over four independent readers.

Characteristics	Reader-1		Reader-2		Reader-3		Reader-4	
	Rec	No Rec	Rec	No Rec	Rec	No Rec	Rec	No Rec
Diagnostic improvement with GBCA								
No, incorrect downgrading of a recurrence	2/21 (9.5)	–	3/21 (14.3)	–	1/21 (4.8)	–	0/21 (0)	–
Yes, downgrading of a scar	–	1/35 (2.9)	–	1/35 (2.9)	–	8/35 (22.9)	–	2/35 (5.7)
Same misdiagnosis	0/21 (0)	2/35 (5.7)	0/21 (0)	1/35 (2.9)	6/21 (28.6)	0/35 (0)	5/21 (23.8)	2/35 (5.7)
Same correct diagnosis	11/21 (52.4)	24/35 (68.6)	12/21 (57.1)	30/35 (85.7)	6/21 (28.6)	26/35 (74.3)	11/21 (52.4)	29/35 (82.9)
No, incorrect upgrading of a scar	–	8/35 (22.9)	–	3/35 (8.6)	–	1/35 (2.9)	–	2/35 (5.7)
Yes, upgrading of a recurrence	8/21 (38.1)	–	6/21 (28.6)	–	8/21 (38.1)	–	5/21 (23.8)	–
Added value of GBCA								
No	13/21 (61.9)	34/35 (97.1)	15/21 (71.4)	34/35 (97.1)	13/21 (61.9)	27/35 (77.1)	16/21 (76.2)	33/35 (94.3)
Yes	8/21 (38.1)	1/35 (2.9)	6/21 (28.6)	1/35 (2.9)	8/21 (38.1)	8/35 (22.9)	5/21 (23.8)	2/35 (5.7)
Total added value	9/56 (16.1)	7/56 (12.5)	16/56 (28.6)	7/56 (12.5)				

Data are proportions of patients with percentages in parentheses (over the total number of recurrences or the total number of simple scars).
Rec indicates recurrence. NoRec indicates no recurrence. GBCA indicates gadolinium-based contrast agent.

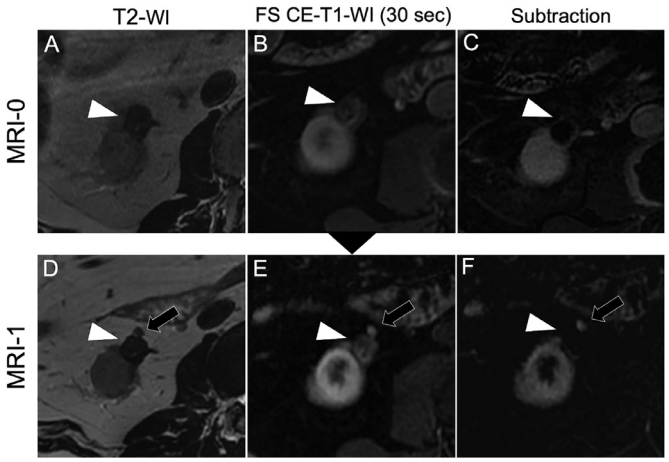

Fig. 4. Added value of gadolinium-based contrast agent to diagnose local recurrence in a 57-year-old man after percutaneous radiofrequency ablation of a grade II, 13-mm, clear cell renal cell carcinoma. Forty-eight months after initial thermal ablation MRI (MRI-0) shows usual ablation zone on T2-weighted image (**A**), fat suppressed (FS) contrast-enhanced (CE) T1-weighted image obtained 30 s after injection (**B**) and (**C**) corresponding subtraction (arrowhead). Twelve months later, MRI-1 demonstrates a new exophytic nodule (arrow) abutting the scar (arrowhead), with intermediate signal on T2-weighted image (**D**), early contrast enhancement (**E**), better seen on subtracted image (**F**). Thus, recurrence was easier to diagnose owing to the use of gadolinium-based contrast agent.

diagnose simple scars was less obvious, as radiologists rarely downgraded their diagnosis (except for Reader-3 in eight 'control' observations). Interestingly, GBCA injection has also led to false positives (*i.e.*, incorrect upgrading of a scar), which occurred for two to eight scars

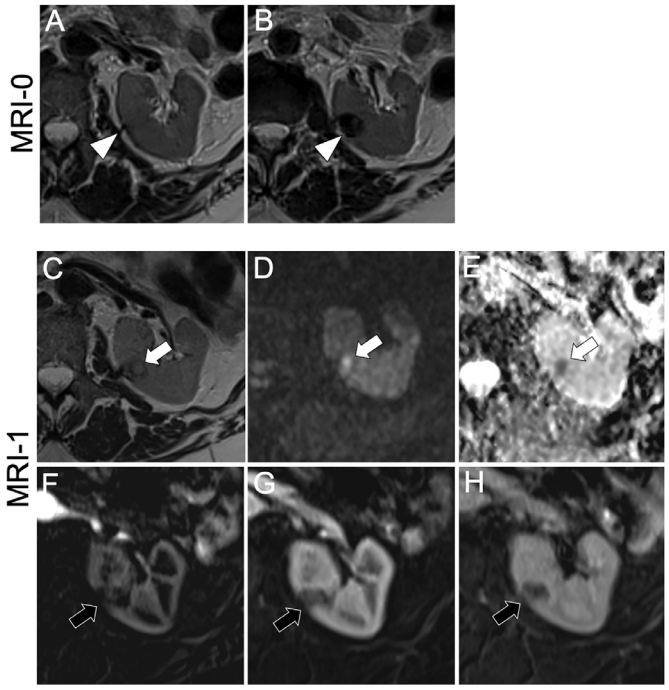

Fig. 5. Example of a recurrence that was correctly diagnosed without requiring gadolinium-based contrast agent in a 75-year-old man after radiofrequency ablation of a grade II, 15-mm, clear cell renal cell carcinoma. Six months after the procedure MRI (MRI-0) demonstrates an usual scar with low signal on T2-weighted image, here on two contiguous slices (arrowheads) (**A, B**). On MRI-1, a new peripheral nodule appeared with intermediate signal intensity on T2-weigted image (**C**), high signal intensity on trace image of the diffusion-weighted image with diffusion restriction on apparent diffusion coefficient map (arrows) (**E**) and was diagnosed as a recurrence. However, this recurrence was poorly visible on subtracted images obtained from dynamic acquisition at 30 s (**F**), 90 s (**G**) and 2–3 min (**H**).

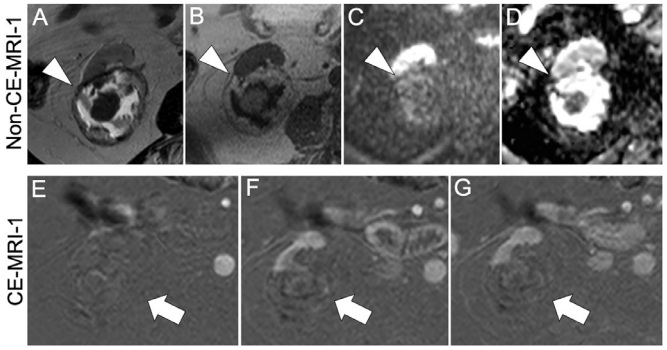

Fig. 6. Added value of gadolinium-based contrast agent to strengthen the diagnosis of a simple scar in a 92-year-old man after cryoablation of a grade II, 32-mm, clear cell renal cell carcinoma. The ablation zone (arrowheads) remained stable in size (64 mm) between MRI at 6 months (MRI-0, not shown) and MRI-1 (performed 6 months later), and demonstrated heterogeneous signal intensities on T2-weighted image (**A**), on T1-weighted image (**B**), no high signal abnormalities on the trace image of the diffusion-wighted image (**C**) but heterogeneous apparent diffusion coefficient values (**D**). Importantly, no contrast enhancement was visible on subtracted images at 30 s (**E**), 90 s (**F**) and 3 min (**G**).

in this study, depending of the reader, which could be explained by the inflammatory changes of the ablation zone [16–19].

The subgroup analyses deepened our understanding of which situations may benefit from intravenous administration of GBCA or not although the small sample sire of our study reduced the scope of our findings. Indeed, it logically seemed more relevant to ask for GBCA injection to follow-up ccRCCs that demonstrated hyper-arterialization on pre-treatment imaging [16–19]. On the opposite, large and heterogeneous ablation zones on T1 and T2- weighted images can be very difficult to analyze and radiologists could appreciate additional CE sequences to strengthen their interpretation.

Although most reviews and guidelines recommend performing regular CE MRIs during the follow-up of patients treated with percutaneous TAs for small renal cancers in order to detect local recurrence and complete treatment, quantitative and objective assessments of the added value of the systematic use of GBCA are lacking [16–18]. With the recent controversies about the long-term consequences of GBCA deposits and given the fact that most T1 ccRCCs are generally cancers of limited aggressiveness, addressing this issue appears even more desirable [23–26]. Herein, using a retrospective case-control design of carefully selected patients treated in a tertiary referral center whose MRI examinations were double-blinded reviewed by four senior radiologists, On average, all diagnostic performance metrics showed trend towards higher values with CE-MRIs compared to non-CE-MRI as well as higher inter-observer reproducibility. However, in details, those differences were rarely significant and more contrasted depending on the radiologists, especially for specificity and accuracy. Furthermore, our subgroup analyses highlighted some situations were injection may be more relevant or possibly omitted. Overall, these findings advocate for a more reasoned use of GBCA on a case-by-case setting.

This study has limitations. It was a retrospective, single-center, case-control investigation on a limited number of examinations obtained on different MRI systems (with subsequent different magnetic fields, acquisition parameters, or GBCAs). It must be noted that we purposely decided to match the numbers of case and control lesions so that accuracy and AUROC and their comparisons were more meaningful metrics but the true rates or recurrence is far lower (5% *vs.* 37.5%). Our reading method (*i.e.*, without delay between interpretation of the non-CE and CE sequences) was chosen in purpose, despite the fact that it is responsible for a learning bias, in order to get as close as possible to the conditions of interpretation of real life. Furthermore, none of the recurrences was confirmed with histologic analysis from biopsy sample. However, diagnoses were validated by

Table 6
Comparisons between recurrences that were correctly diagnosed using gadolinium-based contrast agent and those that were correctly diagnosed without using gadolinium-based contrast agent.

Characteristics	Recurrence		
	Correct diagnosis with GBCA but not without GBCA (n = 8)	Correct diagnosis without GBCA (n = 8)	P-value
Initial tumor characteristics			
Initial tumor size (mm)	29 ± 7 [19–42]	33 ± 12 [18–52]	0.75
Initial tumor grade*			
I	0/8 (0)	1/6 (16.7)	0.54
II	6/8 (75)	4/6 (66.7)	
III	1/8 (12.5)	1/6 (16.7)	
IV	1/8 (12.5)	0/6 (0)	
Initial tumor laterality			
Right	5/8 (62.5)	2/8 (25)	0.31
Left	3/8 (37.5)	6/8 (75)	
Initial tumor location (in depth)			
Exophytic	3/8 (37.5)	3/8 (37.5)	0.45
Endophytic and exophytic	1/8 (12.5)	1/8 (12.5)	
Endophytic	2/8 (25)	4/8 (50)	
Endophytic-endosinusal	2/8 (25)	0/8 (0)	
Initial tumor location (antero-posterior)			
Anterior	2/8 (25)	1/8 (12.5)	0.08
Antero-medial	5/8 (62.5)	1/8 (12.5)	
Postero-medial	0/8 (0)	2/8 (25)	
Posterior	1/8 (12.5)	4/8 (50)	
Initial tumor location (height)			
Equatorial	2/8 (25)	5/8 (62.5)	0.35
Lower side	3/8 (37.5)	1/8 (12.5)	
Upper side	3/8 (37.5)	2/8 (25)	
Intial tumor hyper-arterialization (yes)	7/7 (100)	5/7 (71.4)	0.45
Type of percutaneous treatment			
Cryoablation	3/8 (37.5)	4/8 (50)	0.56
Microwave	1/8 (12.5)	2/8 (25)	
Radiofrequency	4/8 (50)	2/8 (25)	
Characteristics of the treated site			
Size of the scar (mm)	34 ± 10 [24–50]	36 ± 8 [23–46]	0.75
Scar signal on T2-weighted images			
Heterogeneous	5/8 (62.5)	4/8 (50)	>0.99
Low SI	3/8 (37.5)	4/8 (50)	
Iso SI	0/8 (0)	0/8 (0)	
Presence of a peripheral halo on T2W images (yes)	3/8 (37.5)	2/8 (25)	>0.99
Scar signal T1-weighted images			
Heterogeneous	5/8 (62.5)	2/8 (25)	0.13
High SI	0/8 (0)	4/8 (50)	
Low SI	1/8 (12.5)	1/8 (12.5)	
Iso SI	2/8 (25)	1/8 (12.5)	
Enhancement of the treated site (yes)	3/8 (37.5)	3/8 (37.5)	1
Characteristics of recurrence			
Size of the recurrence	22 ± 5 [14–28]	28 ± 11 [17–49]	0.37
Shape of the recurrence			
Crescent	4/8 (50)	1/8 (12.5)	0.28
Nodular	4/8 (50)	7/8 (87.5)	
Recurrence signal on T1-weighted images			
Heterogeneous	0/8 (0)	1/8 (12.5)	0.16
Low SI	0/8 (0)	2/8 (25)	
Iso SI	8/8 (100)	5/8 (62.5)	
T2 signal of the recurrence			
Heterogeneoous	0/8 (0)	1/8 (12.5)	0.17
High SI	0/8 (0)	2/8 (25)	
Low SI	2/8 (25)	0/8 (0)	
Iso SI	6/8 (75)	5/8 (62.5)	
ADC value of recurrence			
High	1/8 (12.5)	1/8 (12.5)	0.23
Iso	2/8 (25)	2/8 (25)	
Not analyzable	3/8 (37.5)	0/8 (0)	
Low	2/8 (25)	5/8 (62.5)	
Enhancement pattern of the recurrence			
Peak and wash-out	6/8 (75)	2/8 (25)	0.07
Peak and plateau	2/8 (25)	3/8 (37.5)	
Slowly progressive	0/8 (0)	3/8 (37.5)	

Quantitative variables are expressed as means ±standard deviations; numbers in brackets are ranges. Qualitative variables are expressed as proportions followed by percentages into parentheses.
ADC indicates apparent diffusion coefficient; GBCA indicates gadolinium-based contrast agent; SI indicates signal intensity.
* Tumor grade is based on Fuhrman classification.

additional follow-up MRI if needed, and by the multidisciplinary tumor board of our university hospital including senior radiologists from our urogenital imaging department. Moreover, two remaining ambiguous observations were excluded to avoid biasing our results.

In conclusion, this study proposes a comprehensive and quantitative assessment of the diagnostic performances, reproducibility, and added value of non-CE sequences from follow-up MRIs after renal percutaneous TAs for small ccRCCs. Although adding CE sequences seems to provide better diagnostic accuracy, our results per radiologist and per subgroups suggest that the systematic use of GBCA could be discussed on a case-by-case basis considering the characteristics of the initial tumor, the ablation zone features and the patient's context, paving the way for a more personalized diagnostic imaging strategy including more homogeneous interpretation practices.

Human rights

The authors declare that the work described has been performed in accordance with the Declaration of Helsinki of the World Medical Association revised in 2013 for experiments involving humans.

Informed consent and patient details

The institutional review board of our institution approved this study. The authors declare that this report does not contain any personal information that could lead to the identification.

Funding

This work did not receive any grant from funding agencies in the public, commercial, or not-for-profit sectors.

Author contributions

All authors attest that they meet the current International Committee of Medical Journal Editors (ICMJE) criteria for Authorship.

Conceptualization: JGD, CM, AC
Data curation: JGD, CM, AC
Formal analysis: AC
Funding acquisition: JCB; NG
Investigation: JGD, CM, AC
Methodology: JGD, CM, AC, NG
Project administration: NG, AC, CM
Resources: JCB, JGD
Software: AC
Supervision: EJ, YLB
Validation: CM, AC
Visualization: CM, AC
Writing – original draft: JGD
Writing – review & editing: CM, AC

Disclosure of Interests

All authors declare no actual or potential conflict of interest related to the submitted study.

References

[1] Shuch B, Amin A, Armstrong AJ, Eble JN, Ficarra V, Lopez-Beltran A, et al. Understanding pathologic variants of renal cell carcinoma: distilling therapeutic opportunities from biologic complexity. Eur Urol 2015;67:85-97.
[2] Ward RD, Tanaka H, Campbell SC, Remer EM. 2017 AUA Renal mass and localized renal cancer guidelines: imaging implications. Radiographics 2018;38:2021-2033.
[3] Ljungberg B, Albiges L, Abu-Ghanem Y, Bensalah K, Dabestani S, Fernández-Pello S, et al. European Association of Urology guidelines on renal cell carcinoma: the 2019 Update. Eur Urol 2019;75:799-810.
[4] Bensalah K, Albiges L, Bernhard JC, Bigot P, Bodin T, Boissier R, et al. AFU guidelines: the 2018-2020 update on management of kidney cancer. Prog Urol 2018;28:5-33.
[5] Escudier B, Porta C, Schmidinger M, Algaba F, Patard JJ, Khoo V, et al. Renal cell carcinoma: ESMO clinical practice guidelines for diagnosis, treatment and follow-up. Ann Oncol 2014;25 iii49-56.
[6] Krokidis ME, Orsi F, Katsanos K, Helmberger T, Adam A. CIRSE guidelines on percutaneous ablation of small renal cell carcinoma. Cardiovasc Intervent Radiol 2017;40:177-191.
[7] Pecoraro A, Porpiglia F, Karakiewicz PIRe, Jack Andrews R, Atwell Thomas, Schmit Grant, et al. Oncologic outcomes following partial nephrectomy and percutaneous ablation for cT1 renal masses. Eur Urol 2019;76:244–51.
[8] Atwell TD, Vlaminck JJ, Boorjian SA, Kurup AN, Callstrom MR, Weisbrod AJ, et al. Percutaneous cryoablation of stage T1b renal cell carcinoma: technique considerations, safety, and local tumor control. J Vasc Interv Radiol 2015;26:792-799.
[9] Pierorazio PM, Johnson MH, Patel HD, Sozio SM, Sharma R, Iyoha E, et al. Management of renal masses and localized renal cancer: systematic review and meta-analysis. J Urol 2016;196:989-999.
[10] Salagierski M, Wojciechowska A, Zając K, Klatte T, Thompson RH, Cadeddu JA, et al. The role of ablation and minimally invasive techniques in the management of small renal masses. Eur Urol Oncol 2018;1:395-402.
[11] Uhlig J, Strauss A, Rücker G, Seif Amir Hosseini A, Lotz J, Trojan L, et al. Partial nephrectomy *versus* ablative techniques for small renal masses: a systematic review and network meta-analysis. Eur Radiol 2019;29:1293-1307.
[12] Cazalas G, Klein C, Piana G, De Kerviler E, Gangi A, Puech P, et al. A multicenter comparative matched-pair analysis of percutaneous tumor ablation and robotic-assisted partial nephrectomy of T1b renal cell carcinoma (AblatT1b study-UroCCR 80). Eur Radiol 2023. doi: 10.1007/s00330-023-09564-6.
[13] De Marini P, Cazzato RL, Garnon J, Dalili D, Leonard-Lorant I, Leclerc L, et al. Safety and oncologic efficacy of percutaneous MRI-guided cryoablation of intraparenchymal renal cancers. Diagn Interv Imaging 2021;102:531-538.
[14] Cornelis FH, Marcelin C, Bernhard JC. Microwave ablation of renal tumors: a narrative review of technical considerations and clinical results. Diagn Interv Imaging 2017;98:287-297.
[15] Autrusseau PA, Boatta E, Cazzato RL, Auloge P, Mayer T, Weiss J, et al. Percutaneous image-guided cryoablation with temporary balloon occlusion of the renal artery for the treatment of central renal tumors. Diagn Interv Imaging 2022;103:510-515.
[16] Campbell SC, Clark PE, Chang SS, Karam JA, Souter L, Uzzo RG. Renal mass and localized renal cancer: evaluation, management, and follow-up: AUA Guideline: part I. J Urol 2021;206:199-208.
[17] Lum MA, Shah SB, Durack JC, Nikolovski I. Imaging of small renal masses before and after thermal ablation. Radiographics 2019;39:2134-2145.
[18] Iannuccilli JD, Grand DJ, Dupuy DE, Mayo-Smith WW. Percutaneous ablation for small renal masses-imaging follow-up. Semin Intervent Radiol 2014;31:50-63.
[19] Patel N, King AJ, Breen DJ. Imaging appearances at follow-up after image-guided solid-organ abdominal tumour ablation. Clin Radiol 2017;72:680-690.
[20] Wile GE, Leyendecker JR, Krehbiel KA, Dyer RB, Zagoria RJ. CT and MR imaging after imaging-guided thermal ablation of renal neoplasms. Radiographics 2007;27:325-339.
[21] Rouvière O, Cornelis F, Brunelle S, Roy C, André M, Bellin MF, et al. Imaging protocols for renal multiparametric MRI and MR urography: results of a consensus conference from the French Society of Genitourinary Imaging. Eur Radiol 2020;30:2103-2114.
[22] Expert Panel on Urological Imaging, Purysko AS, Nikolaidis P, Dogra VS, Ganeshan D, Gore JL, et al. ACR Appropriateness Criteria® post-treatment follow-up and active surveillance of clinically localized renal cell cancer. J Am Coll Radiol 2019;16:S399-416.
[23] de Laforcade L, Bobot M, Bellin MF, Clément O, Grangé S, Grenier N, et al. Kidney and contrast media: common viewpoint of the French Nephrology societies (SFNDT, FIRN, CJN) and the French Radiological Society (SFR) following ESUR guidelines. Diagn Interv Imaging 2021;102:131-139.
[24] McDonald RJ, McDonald JS, Kallmes DF, Jentoft ME, Murray DL, Thielen KR, et al. Intracranial gadolinium deposition after contrast-enhanced MR imaging. Radiology 2015;275:772-782.
[25] Alkhunizi SM, Fakhoury M, Abou-Kheir W, Lawand N. Gadolinium retention in the central and peripheral nervous system: implications for pain, cognition, and neurogenesis. Radiology 2020;297:407-416.
[26] Richter H, Bücker P, Martin LF, Dunker C, Fingerhut S, Xia A, et al. Gadolinium tissue distribution in a large-animal model after a single dose of gadolinium-based contrast agents. Radiology 2021;301:637-642.
[27] Kobayashi M, Levendovszky SR, Hippe DS, Hasegawa M, Murata N, Murata K, et al. Comparison of human tissue gadolinium retention and elimination between gadoteridol and gadobenate. Radiology 2021;300:559-569.
[28] Rogowska J, Olkowska E, Ratajczyk W, Wolska L. Gadolinium as a new emerging contaminant of aquatic environments. Environ Toxicol Chem 2018;37:1523-1534.
[29] Mervak BM, Altun E, McGinty KA, Hyslop WB, Semelka RC, Burke LM. MRI in pregnancy: indications and practical considerations. J Magn Reson Imaging 2019;49:621-631.
[30] Barat M, Jannot AS, Dohan A, Soyer P. How to report and compare quantitative variables in a radiology article. Diagn Interv Imaging 2022;103:571-573.
[31] Robin X, Turck N, Hainard A, Tiberti N, Lisacek F, Sanchez JC, et al. pROC: an open-source package for R and S+ to analyze and compare ROC curves. BMC Bioinformatics 2011;12:77.